

Estimation of Crevice Corrosion Life Time for Stainless Steels in Seawater Environments

Ryo MATSUHASHI*
Yutaka TADOKORO

Shinji TSUGE
Tooru SUZUKI

Abstract

Evaluation results of (1) incubation time of crevice corrosion and (2) growth behavior of stable crevice toward depth direction after initiation are described by measurements of current density vs. potential curves of various stainless steels under constant potential condition in sea water and diluted sea water in order to clarify crevice corrosion life of stainless steels in sea water environments such as brine, brackish water and sea water. Namely, current density vs. potential curves of stainless steel specimens with crevice wet polished just before a measurement is obtained under constant potential condition. And initiation time of crevice corrosion is analyzed by the results, current density vs. potential. Also, relationship between maximum crevice corrosion depth and holding time at constant potential after initiation of crevice corrosion is examined by measurements of crevice corrosion depth and growth of crevice corrosion is quantitatively analyzed by time. In concerning the estimation of crevice corrosion lifetime for ships, component material of offshore structure used in sea water environments, very valuable engineering evidence is obtained and described in this paper.

1. Introduction

Various methods have been studied to evaluate crevice corrosion. Here three representative examples are presented. In one method, several test pieces having a crevice are immersed in natural seawater for a certain period of time, after which the crevices are observed to evaluate the incidence of corrosion¹⁻⁴). In another, the critical temperature at which crevice corrosion occurs in test pieces in a FeCl_3 -based acid solution is measured⁵⁻⁶). In the other, cyclic polarization is applied to measure electrochemically the corroded crevice repassivation potential ($E_{\text{R,CREV}}$) that is the crevice corrosion protective potential⁷). These and many other evaluation methods express

the susceptibility of stainless steels to crevice corrosion in terms of incidence, critical temperature, or potential. However, since they do not evaluate crevice corrosion on a time-serial basis, the evaluation results are, more often than not, difficult to understand intuitively.

Incidentally, according to the $E_{\text{R,CREV}}$ measurements using the controlled potential method as described in the prominent paper by Tsujikawa et al.⁸⁻¹⁰), in the noble potential region before $E_{\text{R,CREV}}$ is reached, the baser the potential, the longer the period in which crevice corrosion occurs (this period is referred to as the “latent period” in the paper¹⁰)). The relevant diagram in the paper contains basic principles for estimating the time in which crevice corrosion will occur with a specific stainless steel material. Thus, the paper pre-

* Senior Researcher, D.Eng., Steel Products Research Lab. -I, Steel Research Laboratories, Nippon Steel Corporation
20-1, Shintomi, Futtsu, Chiba

sents very important experimental results suggesting the possibility of quantitative evaluation of crevice corrosion on a time-serial basis.

In contrast, concerning the behavior of crevice corrosion, specifically the development of crevice corrosion, various studies present: on-site crevice corrosion measurements using the moiré method; basic knowledge, including the rate of metal dissolution¹¹⁾, the movement of relevant substances, the condition of potential distribution¹²⁾, and the change in pH of the analyte in the crevice¹³⁾; the average rate of metal dissolution in the crevice measured by a controlled potential test in which the crevice anode and the free-surface cathode are separated from each other¹⁴⁾, etc.

However, there are no reports on a detailed and systematic study of the macroscopic time-serial change in the depth of crevice corrosion of various types of stainless steel that is effective in engineering. From the standpoint of the service life of structures, there are no particular problems as long as the rate of development of crevice corrosion is sufficiently low. Therefore, field exposure tests on stainless steels in river water, dam reservoirs, brackish water and seawater have been conducted by the government agencies concerned¹⁵⁾, etc. Nevertheless, there are few reports on the underlying logic of depth-wise development of crevice corrosion of various types of stainless steels.

In this paper, which focuses on electrochemical evaluation of crevice corrosion of various stainless steels in a seawater-based environment, we describe a method of evaluating the life of stainless steels which are subject to crevice corrosion based on a current-time curve obtained by the controlled potential method from the standpoint of the time of occurrence and the development of crevice corrosion, together with the evaluation results obtained by the above method.

2. Steels Tested and Test Method

2.1 Steels tested and test pieces

Five steel grades—SUS304, SUS316L, SUS329J₄L, NSSC250 and NSSC270—were tested. The representative chemical composition and *CI* value ($CI = [Cr] + 4.1[Mo] + 27[N]^{16)}$ of each of those steels are shown in **Table 1**. All the steels tested were solution heat-treated materials (3- to 6-mm thick) commonly available on the market.

To study the mechanism by which crevice corrosion occurs and its developmental behavior, we prepared test pieces provided with a crevice as shown in **Fig. 1**. Each of the test pieces consisted of two steel sheets—one measuring 20 mm (W) × 50 mm (L) × 3 mm (T) and the other measuring 20 mm (W) × 20 mm (L) × 3 mm (T). After steel samples were collected in such a manner that the rolled surface became the test surface, the entire test piece surface was wet-ground to #400 and an enameled lead wire was soldered to the top end of the longer sheet. After that, the test piece was immersed in 30% HNO₃ solution at 50°C for one hour for passivation. Immediately before the prescribed electrochemical measurement was started, the test surface (i.e., the interface between the 20 mm × 50 mm sheet and the 20 mm × 20 mm sheet; hereinafter referred to as the

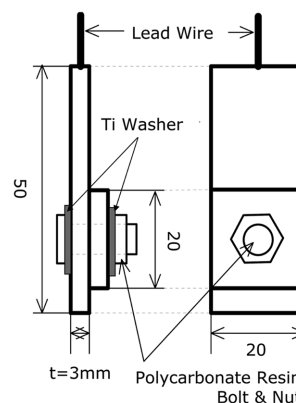


Fig. 1 Schematic illustration of specimen with crevice

crevice) was wet-ground to #400 again. With the test solution applied to the test surface, the two sheets were fitted together with polycarbonate resin nuts and bolts and titanium washers as shown in **Fig. 1**. (This combination of two sheets is hereinafter referred to as the test piece with a crevice.)

In conducting the present test, there was concern that the titanium washers would have some effect on the electrochemical measurement system. Therefore, we measured the time-serial change in natural potential and conducted a controlled potential test with and without the titanium washers. As a result, it was confirmed that as far as the natural potential and the current density-time curve are concerned, the titanium washers made no significant difference. The electrochemical measurement was performed with each test piece with a crevice immersed in the test solution in such a manner that the solution level in the cell reached a point 10 mm from the top end of the test piece. Under that condition, the total area of the test piece measured was about 28.1 to 30.5 cm² and the crevice area was about 7.43 cm².

2.2 Test solutions

The test solutions used were ASTM artificial seawater (D-1141-52) and Cl⁻ solutions of different concentrations obtained by diluting the artificial seawater 10 to 1,000 times with pure water. (These test solutions are hereinafter referred to as the seawater-based solutions.) Although details are omitted here, the Cl⁻ concentrations were in the range of 19 ppm to 18,900 ppm.

2.3 Electrochemical measurement

2.3.1 Measurement of repassivation potential of crevices corrosion

We measured the repassivation potential of crevices corrosion, $E_{R,CREV}$, in accordance with JIS G 0592⁷⁾. The concept of the polarization operation used in the measurement is shown in **Fig. 2**. The value of $E_{R,CREV}$ at 50°C was measured. Concretely, after the test piece with a crevice was de-aerated using Ar (flow rate: 200 ml/min), it was immersed in a 50°C seawater-based solution to measure its one-hour immersion potential. After that, as shown in **Fig. 2**, the immersion potential was polarized toward the anode using the potentiokinetic

Table 1 Main chemical compositions (wt%) and crevice corrosion resistance index *CI* of tested stainless steels

	Cr	Ni	Mo	Cu	N	<i>CI</i>
SUS304	18.20	8.05	-	0.21	-	18.20
SUS316L	17.54	12.08	2.18	0.222	0.02	26.48
SUS329J ₄ L	25.09	7.20	3.03	0.47	0.150	41.56
NSSC250	24.99	17.91	2.45	0.29	0.29	42.87
NSSC270	20.32	17.99	6.18	0.79	0.22	51.60

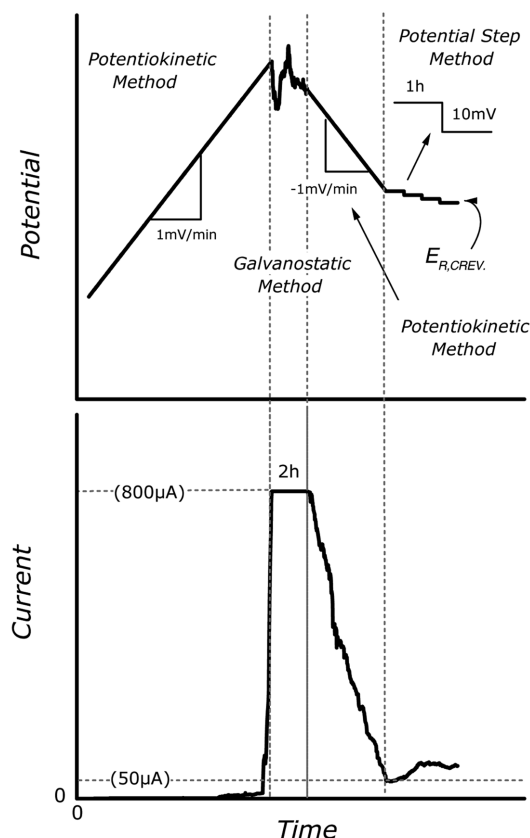


Fig. 2 Operation of polarization method

method (potential sweep rate: 1 mV/min). When the anode current reached $800 \mu\text{A}$, the potential was so controlled that the anode current was maintained at $800 \mu\text{A} \pm 1 \mu\text{A}$ for two hours.

Next, the potential was polarized toward the cathode until the anode current decreased to $50 \mu\text{A}$ using the potentiokinetic method (potential sweep rate: 1 mV/min). The potential at the time the anode current decreased to $50 \mu\text{A}$ was maintained for one hour. This series of operations was repeated until the current flowing one hour later became smaller than the current that flowed one hour earlier. $E_{R,CREV}$ was expressed as the value of the noblest potential at which the current flowing to the test piece electrode stopped increasing at the final stage of the above polarization operation⁷⁾. After the test, the crevice of each of the test pieces was observed under an optical microscope, and those test pieces whose maximum crevice corrosion depth was smaller than $40 \mu\text{m}$ were excluded from consideration in the calculation of $E_{R,CREV}$.

2.3.2 Measurement of time in which crevice corrosion occurred

The test consisted mainly of current density-time curve measurement using the potentiostatic method. In the test, potentiostatic electrolytic equipment (Tohogiken, Inc.'s Model 2000) was used. With an Ag/AgCl electrode: SSE (25°C , +199 mV on SHE basis) in saturated KCl solution used as the reference electrode, potentials in the range of 0 to 700 mV (hereinafter all potentials, expressed in mV, are on an SSE basis) were applied to the test piece electrode and the time-serial change in density of the current flowing to the test piece electrode was measured continuously for one to 360 hours. The potentiostatic test of each test piece was started at the time when the natural potential stabilized within the prescribed range after immersion of the test piece electrode in the test solution. All the tests were

conducted at a temperature of 50°C . Throughout the test, Ar gas was blown into the cell for electrochemical measurement from above. Each of the current values obtained from the tests was divided by 29.4 cm^2 —the total area of the test piece surface that was in contact with the test solution—to convert it into an apparent current density.

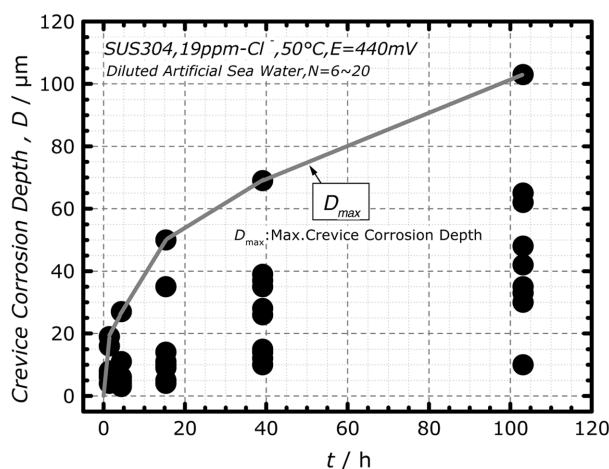
2.3.3 Measurement of development of crevice corrosion

The test pieces with a crevice mentioned earlier (the interfaces were ground immediately before the test) were subjected to a potentiostatic test for about 0.25 to 12 hours arbitrarily at $E_{sp} = 440 \text{ mV}^{17)}$ —the natural potential that ordinary stainless steel shows in a natural water environment. Immediately after the potentiostatic test was conducted for the prescribed time, the test piece was removed from the seawater-based solution and the crevice of the test piece electrode was opened. After the test piece was washed in water and air-dried, the depth of the crevice corrosion that had occurred on the $20 \text{ mm} \times 50 \text{ mm}$ sheet (i.e., the larger sheet of the test piece) was measured under an optical microscope using the focal depth method.

Namely, as shown in Fig. 3, for each of the potential retention times, crevice corrosion depths were measured at several to 20 points to determine the deepest crevice corrosion (max crevice corrosion depth: D_{max}). In this measurement, the test piece interior at least 1.5 mm from the end of the crevice was measured. For the above electrochemical measurements, an Ag/AgCl (25°C , SHE = +199 mV: SSE) electrode in saturated KCl solution was used as the reference electrode.

2.4 Emersion test in natural seawater

Test pieces with a crevice of exactly the same shape as those used in the electrochemical measurement were subjected to an immersion test in natural seawater off the coast of Futtsu City in Chiba Prefecture to study the time-serial change in natural potential of the test pieces. In addition, larger test pieces were subjected to a long-term, semi-immersion test in seawater. In the above immersion test, the test pieces with a crevice were immersed in equipment for immersion tests in natural seawater (Fig. 4) to obtain the natural potential of the stainless steel in a passive state in natural seawater. In the long-term, semi-immersion test, test pieces, each having a couple of crevices, were exposed to the open air and the seawater. (Details of this test are omitted.)

Fig. 3 Measurement of D_{max}

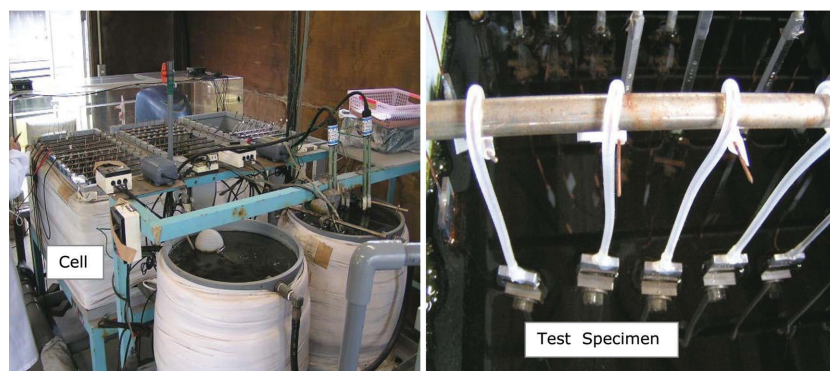


Fig. 4 Equipments of natural sea water immersion test

3. Test Results and Discussions

3.1 Time-serial change in natural potential in natural seawater

Fig. 5 shows the time-serial changes in the natural potential of various stainless steels measured in natural seawater (for about 50 days). All the stainless steels, except SUS304, show very similar time-serial changes in natural potential. Namely, in the early stages of the immersion test, they show a relatively base potential in the range -330 to -50 mV. With the lapse of time, however, their natural potential rapidly shifts toward the noble potential. In about 30 days, it becomes as noble as about 440 mV, and remains almost the same after that. Since the stable natural potential is around 440 mV for all the stainless steels tested (except SUS304), 440 mV is the natural potential, E_{sp} , when the passive state of those steels is stably maintained. In the case of SUS304, by contrast, the natural potential is the base from the early stages of the immersion test. Therefore, the passive state of the steel breaks down relatively early, causing the natural occurrence of crevice corrosion.

3.2 Susceptibility to natural occurrence of crevice corrosion

Fig. 6 shows the polarization curves of SUS316L, SUS329J₄L, NSSC250 and NSSC270 in 30°C natural seawater. The value of the repassivation potential $E_{R,CREV}$ of the corroded crevice was -130 mV for SUS316, -123 mV for SUS329J₄L, -80 mV for NSSC250 and -58 mV for NSSC270.

The repassivation potential, $E_{R,CREV}$, of the corroded crevice means that there is the possibility that crevice corrosion will continue when the potential is nobler than $E_{R,CREV}$, whereas there is little possibility of this when the potential is baser than $E_{R,CREV}$. Thus, $E_{R,CREV}$ is a sort

of yardstick of the corrosion resistance of steel material in terms of the quasi-equilibrium theory. Namely, for any given crevice shape, environmental conditions (Cl^- concentration, temperature, etc.) and steel material, the $E_{R,CREV}$ assumes a specific value, that is, the corrosion resistance of the material (this is called the material force).

In contrast, the natural potential, E_{sp} , shown in Fig. 5 is determined not by the material but by the environmental corrosiveness (this is called the environmental force). Namely, as long as a specific stainless steel remains in a stably passive state, the value of E_{sp} is almost determined by the types and concentrations of the oxidizing substances contained in the environment (diss O_2 , Fe^{3+} , Cu^{2+} , Cr^{6+} , etc.) and the ambient temperature. According to the above logic, it is possible to determine the possibility of crevice corrosion continuing in the environment to which a specific material is exposed; that is, to judge the susceptibility of the material to the natural occurrence of crevice corrosion, by comparing the environmental force with the material force.

Fig. 7 shows the effect of Cl^- concentration on $E_{R,CREV}$ for various stainless steels. In the figure, the values of natural potential E_{sp} obtained by actual measurements under different natural environments are also shown. The condition under which crevice corrosion naturally occurs is as follows.

$$E_{R,CREV} < E_{sp} \quad (1)$$

Therefore, in natural seawater, any stainless steel is sooner or later subject to crevice corrosion, which is supposed to increase with the lapse of time. However, the results of the above measurements do not reveal when crevice corrosion will actually occur. In order to determine the crevice corrosion resistance of each of the stainless steels tested, we estimated the time at which crevice corrosion would naturally occur (crevice corrosion occurrence time) with each stainless steel in a seawater-based environment by using the potentiostatic method. The estimation results are described below.

3.3 Estimation of crevice corrosion occurrence time

As an example, Fig. 8 shows the current-time curves at different temperatures, obtained by the potentiostatic electrolysis of SUS329J₄L at $E = 440$ mV, which is the natural potential (environmental force) of the steel in seawater.

Initially, all the current-time relationships show a downward curve at any temperature with the lapse of electrolytic time. However, at a specific point, which differs according to temperature, the current density begins to increase. This increase in current density directly indicates the occurrence of crevice corrosion on the steel. The time at which the current density begins to increase is the time at which crevice corrosion occurs. (This time is hereinafter referred to as the crevice corrosion occurrence time, t_{INC} .) In the case of SUS329J₄L,

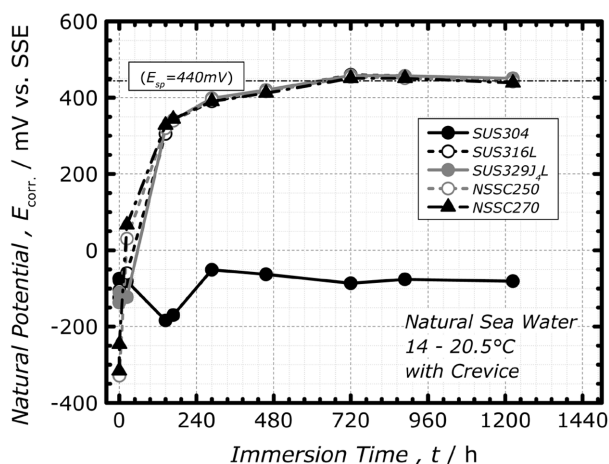


Fig. 5 Potential-time curves of stainless steels in natural sea water

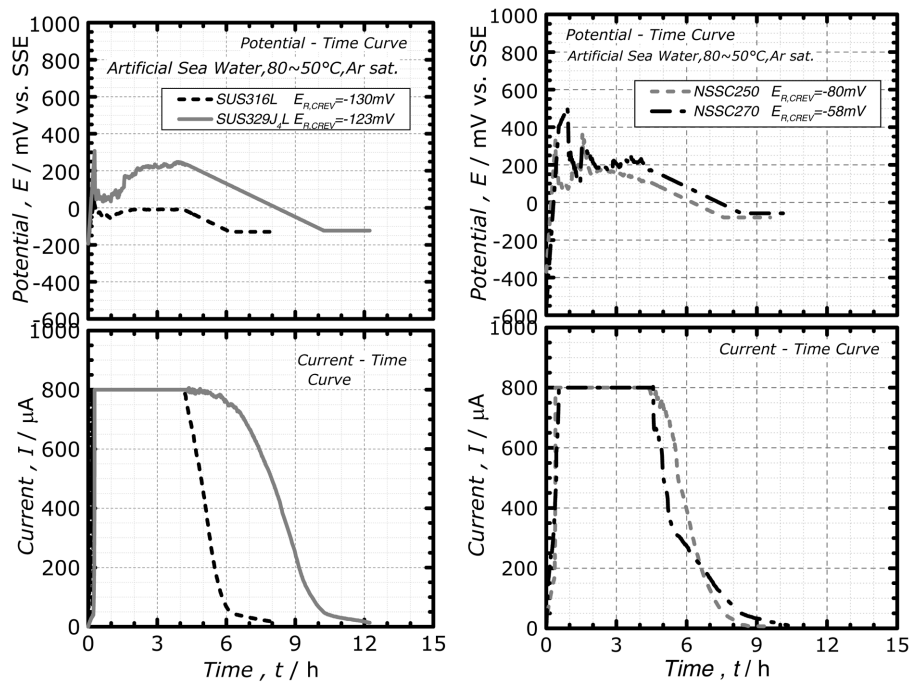


Fig. 6 Polarization curves of various stainless steels

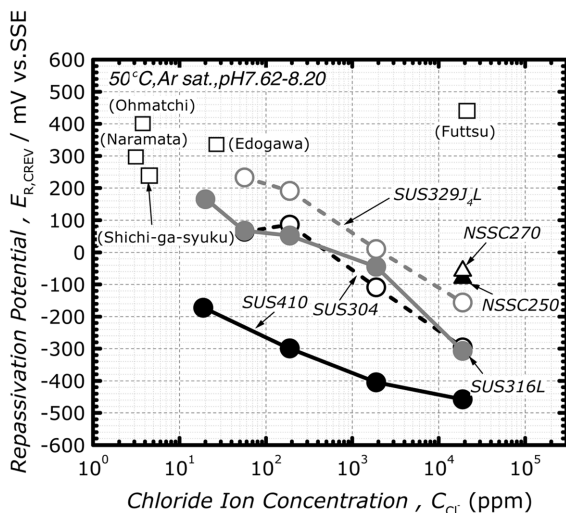


Fig. 7 Effects of Cl^- concentration on $E_{R,CREV}$ for various stainless steels

$t_{\text{INC}}^{\text{INC}}$ decreases with the rise in temperature. This clearly indicates that at higher temperatures, crevice corrosion of the steel occurs more easily.

Fig. 9 shows the effect of Cl^- concentration on crevice corrosion occurrence time ($t_{\text{INC}}^{\text{INC}}$) of the stainless steels tested. The $t_{\text{INC}}^{\text{INC}}$ value of the stainless steels, except NSSC250 and NSSC270, decreased with the increase in Cl^- concentration in the seawater. In contrast, NSSC250 and NSSC270 showed excellent resistance to crevice corrosion. Even when the temperature was as high as about 50°C, they were free from crevice corrosion during measurement of their current-time curves.

The values of $t_{\text{INC}}^{\text{INC}}$ shown in Fig. 9 were obtained by laboratory testing. They are different from the absolute $t_{\text{INC}}^{\text{INC}}$ values for the stainless steels in the actual environment. Ultimately, there are several

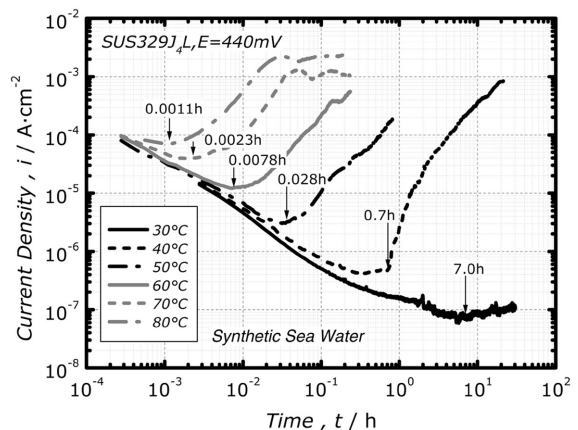


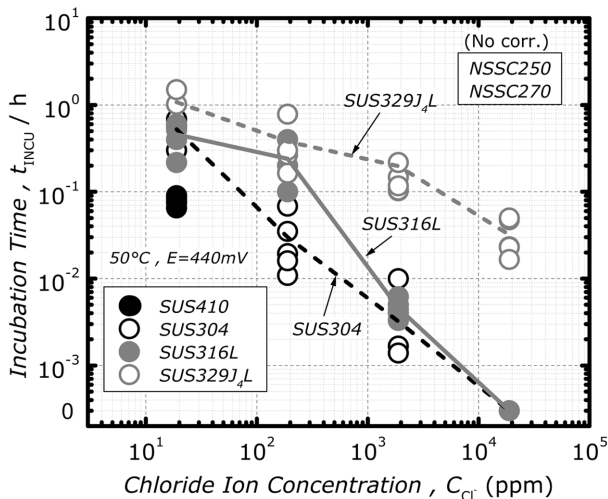
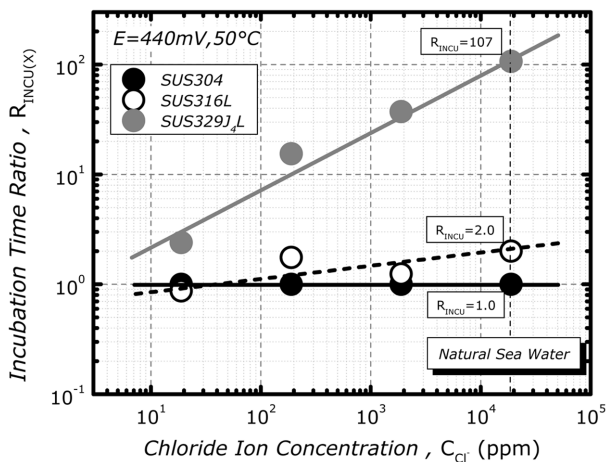
Fig. 8 $i-t$ curves of various temperature (SUS329J₄L)

unpredictable or unavoidable factors, such as the shape of crevices in actual offshore structures and the seasonal change in the seawater temperature. Therefore, it is meaningless to discuss the absolute value of $t_{\text{INC}}^{\text{INC}}$. From an engineering standpoint, it is more meaningful to evaluate the $t_{\text{INC}}^{\text{INC}}$ of each individual stainless steel in comparison with the $t_{\text{INC}}^{\text{INC}}$ of, for example, general-purpose SUS304 in natural seawater.

So, let us define the relative value of $t_{\text{INC}}^{\text{INC}}$ of any stainless steel when compared with the $t_{\text{INC}}^{\text{INC}}$ of SUS304 as $R_{\text{INC}}^{\text{INC}}(X)$ (where X indicates any stainless steel other than SUS304). Then, $R_{\text{INC}}^{\text{INC}}(X)$ can be expressed as follows.

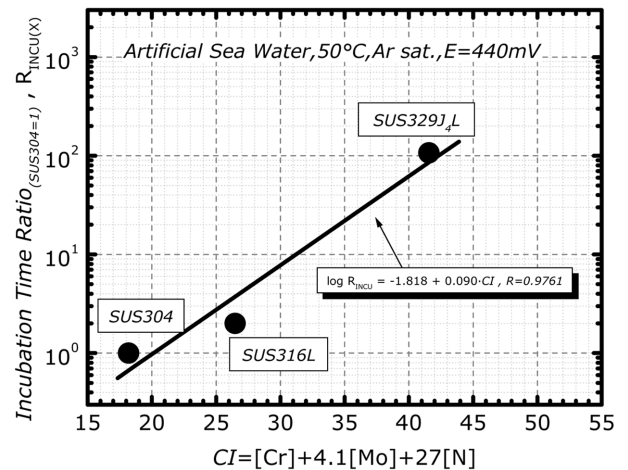
$$R_{\text{INC}}^{\text{INC}}(X) = t_{\text{INC}}^{\text{INC}}(X) / t_{\text{INC}}^{\text{INC}}(\text{SUS304}) \quad (2)$$

Fig. 10 shows the effect of the Cl^- concentration on $t_{\text{INC}}^{\text{INC}}$ of various stainless steels at 50°C expressed as $R_{\text{INC}}^{\text{INC}}$ by using Equation (2) above. The $R_{\text{INC}}^{\text{INC}}$ value for SUS304 is 1.0 regardless of the Cl^- concentration. The effect of the Cl^- concentration on $R_{\text{INC}}^{\text{INC}}$ of SUS316L


 Fig. 9 Effects of Cl^- concentration on t_{INCU} (50°C, $E = 440\text{mV}$)

 Fig. 10 Effects of Cl^- concentration on $R_{\text{INCU}}(X)$

is negligible: at a Cl^- concentration equivalent to that of natural seawater, $R_{\text{INCU}} = 2.0$. This means that in a given period of time, SUS316L is about half as susceptible to crevice corrosion as SUS304. In the case of SUS329J₄L, R_{INCU} increases with the increase in Cl^- concentration. At a Cl^- concentration equivalent to that of natural seawater, the steel is about 107 times less susceptible to crevice corrosion than SUS304.

Thus, we considered that it would be possible to roughly estimate the crevice corrosion occurrence time of any stainless steel in natural seawater by comparing its R_{INCU} with the R_{INCU} of SUS304. In seawater of normal temperature, there is the possibility that crevice corrosion will occur even with NSSC250 and NSC 270 as shown in Fig. 7. However, it has been clarified that an extremely long time is required before crevice corrosion occurs in these steels in a controlled potential electrolysis test. Therefore, we estimated the crevice corrosion occurrence time of these two stainless steels with excellent corrosion resistance, as follows. First, it is assumed that the relationship between R_{INCU} and CI obtained with SUS304, SUS316L and SUS329J₄L as shown in Fig. 11 will be maintained even when the CI value is larger. The relationship shown in Fig. 11 can be expressed as follows.


 Fig. 11 Relationship between the $R_{\text{INCU}}(X)$ and CI value

$$\log R_{\text{INCU}} = -1.818 + 0.090 \cdot CI, R = 0.9761 \quad (3)$$

In contrast, it has been reported that in an exposure test of SUS304 in actual seawater, crevice corrosion occurred on the steel in about one year.¹⁸⁾ From this test result, by using R_{INCU} and Equation (3) above, it is possible to estimate the unknown crevice corrosion occurrence time of any highly corrosion-resistant stainless steel in actual seawater. Assuming the estimated crevice corrosion occurrence time in actual seawater as t_x , the following equation can be obtained.

$$\log (t_x/y) = -1.818 + 0.090 \cdot CI \quad (4)$$

The results of calculations using the above equation are shown in Fig. 12 and Table 2. We assume that once crevice corrosion has occurred in a structure, it will continue growing and ultimately perforate the structure. (Actually, with the development of crevice corrosion, the crevice expands and the conditions inside the crevice become close to the ambient conditions. As a result, it becomes difficult for the crevice corrosion to continue.) Assuming that the functional life of any material is determined by the length of time in which the material is perforated by crevice corrosion, it is extremely important to clarify the resistance of each type of stainless steel to perforations caused by crevice corrosion. In the following subsection, we describe the results of estimation by a controlled potential electrolysis test of the development of crevice corrosion on various stainless steels in seawater.

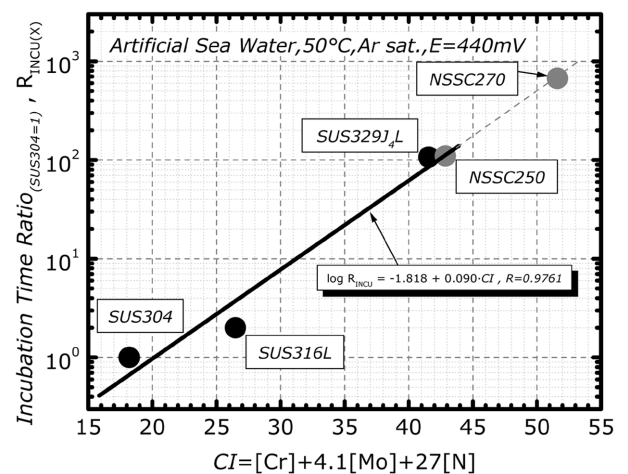

 Fig. 12 Estimation of R_{INCU} for NSSC250 and NSSC270

Table 2 Relationship between the *CI* value and *R*_{INC} for various stainless steels (50°C, *E* = 440mV)

	SUS304	SUS316L	SUS329J ₄ L	NSSC250	NSSC270
<i>CI</i> value ^{*1}	18.20	26.48	41.56	42.87	51.60
<i>t</i> _{INC} (experiment)	0.00014h	0.00028h	0.015h	-	-
<i>t</i> _{INC} (sea water)	1y	-	-	-	-
<i>R</i> _{INC(X)} ^{*2}	1	2	107	-	-
Estimation value ^{*3}	0.66y	3.67y	84y	110y	670y

^{*1}: *CI* = [*Cr*] + 4.1[*Mo*] + 27[*N*], ^{*2}: *R*_{INC(X)} = *t*_{INC(X)} / *t*_{INC(SUS304)}, ^{*3}: Calculation from Equation (4)

3.4 Analysis of development of crevice corrosion

3.4.1 Behavior of metal dissolution in crevice

Fig. 13 shows the current-time curves for SUS304 test pieces with crevices, obtained in a 190-ppm Cl⁻ environment at *E* = 440 mV with the measurement time varied. Each of the current-time curves shows that in the early stages of electrolysis, the current decreases with the lapse of time. However, at a certain period of time, the current begins to increase with the lapse of time. At that time, the test piece showed a series of behaviors indicating that crevice corrosion was progressing. The time at which the current begins to increase after the start of electrolysis is the approximate time required for crevice corrosion to occur (*t*_{INC}). Details of *t*_{INC} have already been discussed.

Fig. 14 shows the conditions and binary (black & white) images of the crevice interfaces of 20 mm × 20 mm sheets at the final electrolysis time positions, (a) - (e), on the current-time curves shown in Fig. 13. Here, *t* - *t*_{INC} represents the difference between the electrolysis time and the crevice corrosion occurrence time; that is, the time elapsed after the occurrence of crevice corrosion (this time is equivalent to the time at which crevice corrosion accelerates). Thus, Fig. 14 gives a concrete illustration of dissolved metallic parts (the black parts in the binary images).

The dissolved metallic parts tend to expand with the increase in (*t* - *t*_{INC}). Namely, as is evident from the influence of crevice corrosion growth time (*t* - *t*_{INC}) on the approximate value, *S*_{CREV}, of the crevice corrosion area of each type of stainless steel after the controlled potential electrolysis test shown in Fig. 15, the larger the value of (*t* - *t*_{INC}) and the higher the Cl⁻ concentration, the larger the value of *S*_{CREV} becomes, regardless of stainless steel type. This behavior suggests that unlike ordinary pitting which grows preferentially in the direction of material thickness, crevice corrosion grows not only in the thickness direction but also over a wide area of the material surface.

Fig. 16 shows the influence of (*t* - *t*_{INC}) on the current density (*i*_{CREV})—the current at the final time position on each of the current-time curves shown in Fig. 13 divided by *S*_{CREV}. With all the stainless steels tested, the higher the Cl⁻ concentration, the larger the value of *i*_{CREV} becomes. In contrast, with the decrease in value of (*t* - *t*_{INC}), the value of *i*_{CREV} gradually increases. The value of *i*_{CREV} measured here is the average density of current flowing through the entire *S*_{CREV}. Actually, however, considering the fact that the depth of crevice corrosion differs from one point to another (in terms of area) as described later, it is estimated that the concentration and pH of the analyte and the rate of metal dissolution will differ within the *S*_{CREV}. In the present study, however, this problem was omitted from consideration.

3.4.2 Time-serial change in maximum crevice corrosion depth

Fig. 17 shows an example of the measurement of maximum depth *D*_{max} of crevice corrosion using an optical microscope. The measure-

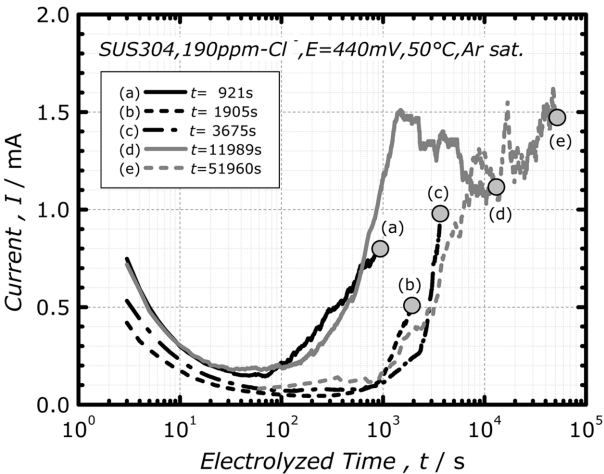


Fig. 13 Growing behavior of crevice corrosion over current-time curves

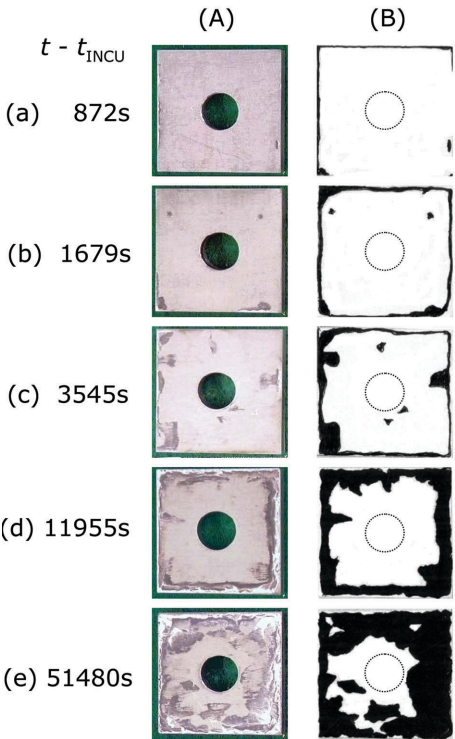
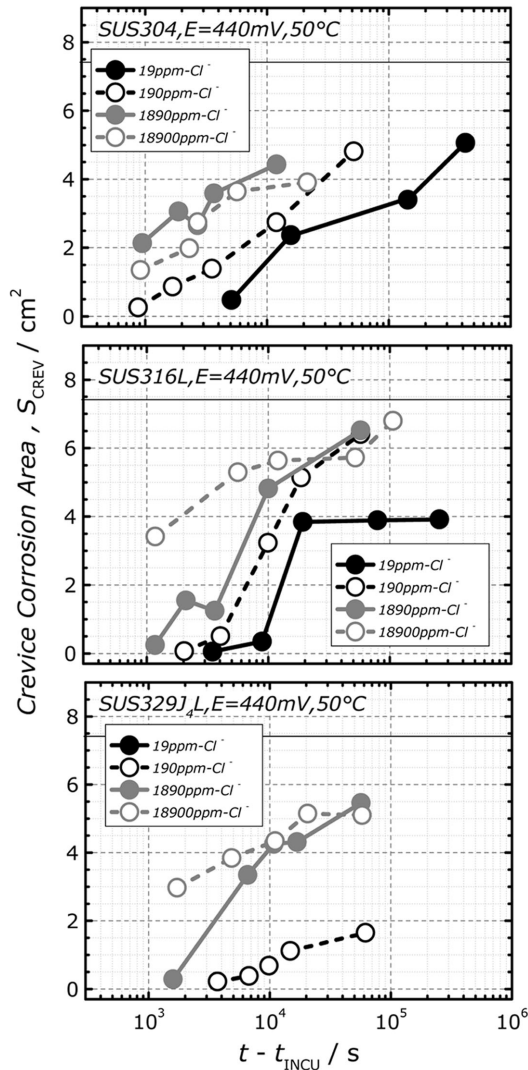
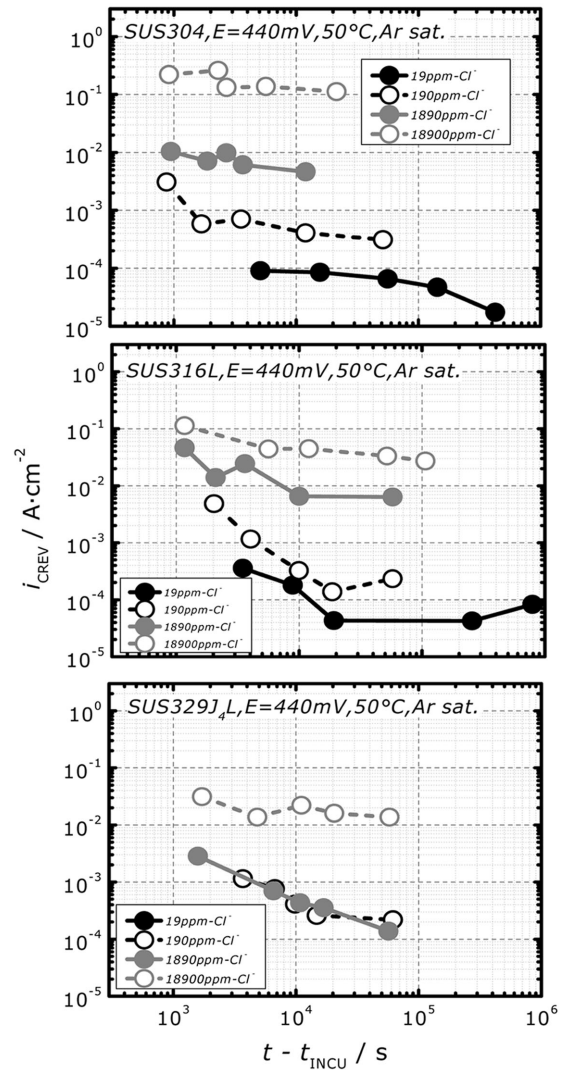


Fig. 14 Time dependence of corrosion area in crevice

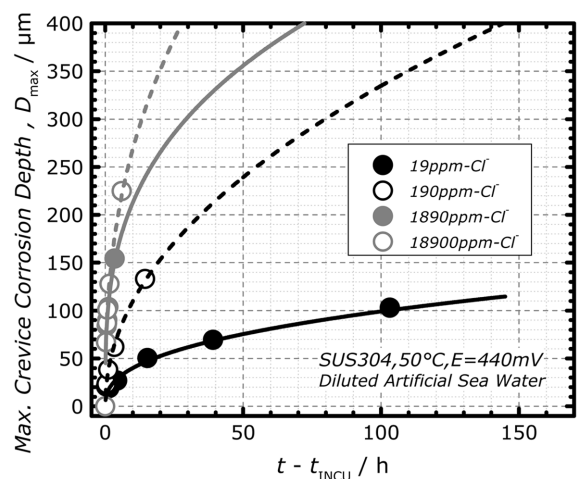
ment was performed as follows. SUS304 test pieces with crevices were held in seawater-based environments of various Cl⁻ concentra-


 Fig. 15 Time dependence of S_{CREV}

 Fig. 16 Time dependence of i_{CREV}

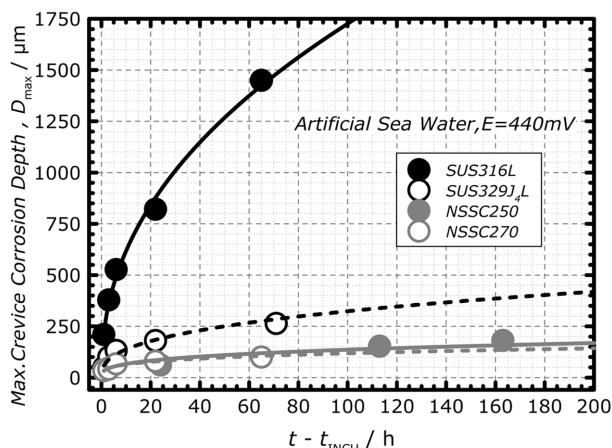
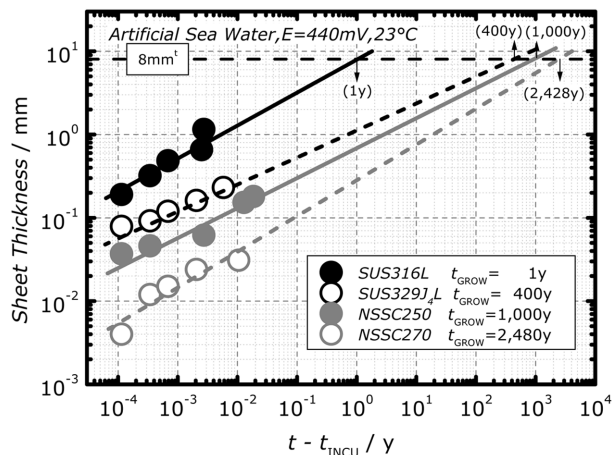
tions with the test piece potential, E , maintained at 440 mV. After the prescribed time, the metal was removed from the interface of each test piece and the depth of crevice corrosion of the metal was measured. For each of the test pieces, crevice corrosion depth was measured at about 20 points and the largest of the measured values, that is, the maximum crevice corrosion depth, D_{max} , was extracted. Next, the values of D_{max} obtained were plotted against total electrolysis time t minus crevice corrosion occurrence time t_{INCUB} (i.e., $(t - t_{\text{INCUB}})$; this time actually corresponds to the crevice corrosion growth time, t_{GROW}). In this way, the D_{max} behavior for various stainless steels in seawater against time was analyzed. As a result, it was found that D_{max} changes power-functionally against $t - t_{\text{INCUB}}$. Therefore, assuming the specific function indicating the growth of crevice corrosion shown in Equation (5) as follows, we obtained the values of constants A and m .

$$D_{\text{max}} = A \cdot (t - t_{\text{INCUB}})^m \quad (5)$$

Fig. 18 shows the dependence on $t - t_{\text{INCUB}}$ of D_{max} of various stainless steels in seawater. With all the stainless steels, the behavior of D_{max} against $t - t_{\text{INCUB}}$ changes power-functionally, suggesting that Equation (5) above is valid. Since D_{max} directly corresponds to the stainless steel sheet thickness ($S.T.$), the following equation can be


 Fig. 17 Example of time dependence of D_{max}

obtained by assuming $D_{\text{max}} = S.T.$ and transforming Equation (5) above into a logarithmic equation.

Fig. 18 Time dependence of D_{\max} for various stainless steelsFig. 19 Estimation results of t_{GROW} in artificial sea water

$$\log (S.T./\text{mm}) = A + m \cdot \log (t - t_{\text{INCU}} / y) \quad (6)$$

Here, y is the unit of time and mm denotes sheet thickness.

The results of calculations using Equation (6) above are plotted in Fig. 19. On the assumption that the sheet thickness ($S.T.$) required of a specific structure was 8 mm, the time in which crevice corrosion would penetrate the sheet (i.e., the time that elapses after the occurrence of crevice corrosion) was estimated from the above results. The estimated time for crevice corrosion to penetrate an 8-mm-thick stainless steel sheet was about one year for SUS316L, about 400 years for SUS329J₄L, about 1,000 years for NSSC250 and about 2,480 years for NSSC270. Thus, with NSSC250 and NSSC270, even when crevice corrosion occurs on an 8-mm-thick sheet, it would not penetrate the sheet in 1,000 years or so. In fact, penetration of the sheet by crevice corrosion is beyond the realm of possibility.

3.5 Crevice corrosion life of various stainless steels in seawater

As has been described above, even stainless steels with excellent corrosion resistance are not completely free from crevice corrosion in seawater. However, their resistance to crevice corrosion is remarkable. In the case of NSSC250, for example, it takes some 110 years for crevice corrosion to occur on it. Moreover, in order for the crevice corrosion to grow and ultimately penetrate an NSSC250 sheet 8-mm thick, for example, would take 1,000 years or so. Thus, the total perforation time—the period from the time when the NSSC250 sheet is put to use until the time when the sheet is penetrated by crevice

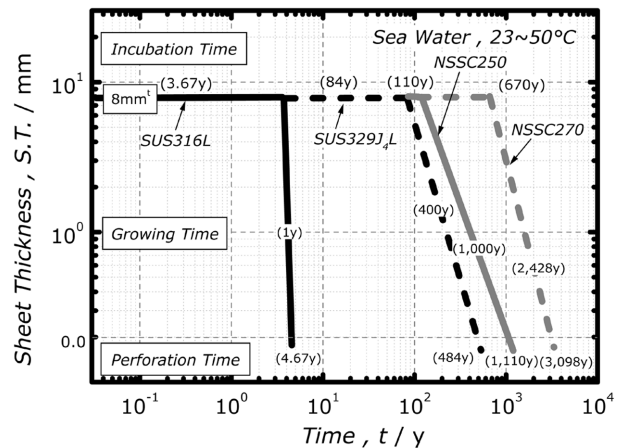


Fig. 20 Crevice corrosion life time for various stainless steels in sea water

corrosion—is estimated to be 1,110 years, or about 11 centuries. From the standpoint of practice and social common sense, as long as NSSC250 is used in seawater of normal temperature, it would be completely free of any problems caused by crevice corrosion.

It should be noted, however, that the information above is based on the results of an estimation of crevice corrosion resistance of stainless steels in the laboratory. In the actual marine environment, there are a number of uncertain and unavoidable factors, such as the formation of a crevice structure by deposition of marine life, damage to the offshore structure caused by objects adrift in the sea, and seasonal weather changes. After all, the crevice corrosion life of stainless steels estimated in the present study is based on the assumption that there were no such factors as mentioned above and that the present test conditions and crevice structure would remain the same forever. Fig. 20 shows the crevice corrosion life, or the perforation time, of various stainless steels, the sum of the estimated crevice corrosion occurrence time described in the preceding subsection and the time required by crevice corrosion to penetrate an 8-mm-thick steel sheet described in this subsection.

3.6 Results of semi-immersion test in natural seawater

Test pieces which had two crevices, one exposed to natural seawater and one exposed to the air, were subjected to a semi-immersion test for 283.4 days (6,808 hours). Fig. 21 shows the results of observation from the air of the test pieces after the test. The test pieces were set in position in such a manner that the bottom end of the crevice exposed to the air always reached the level of the seawater so that the seawater infiltrated the crevice by capillary action. In the case of SUS316L and SUS329J₄L, rust can be observed by the naked eye not only on the free surface of the flat part, but also on the crevice. By contrast, NSSC250 shows no signs of corrosion on the free surface of the flat part or on the crevice, indicating that it has superior corrosion resistance. Fig. 22 shows the conditions of the surfaces of the test pieces that were taken out of the seawater after the test and removed of deposits on the surface.

SUS316L shows relatively conspicuous corrosion on both the crevice immersed in the seawater and the crevice exposed to the air. In the case of SUS329J₄L, the crevice exposed to the air reveals corrosion, although the crevice immersed in the seawater is free of corrosion. In contrast, NSSC250, NSSC270 and other stainless steels with excellent corrosion resistance (but not shown in Fig. 22) were completely free from corrosion and rust on the crevice immersed in the seawater and the crevice exposed to the air. Thus, they demon-

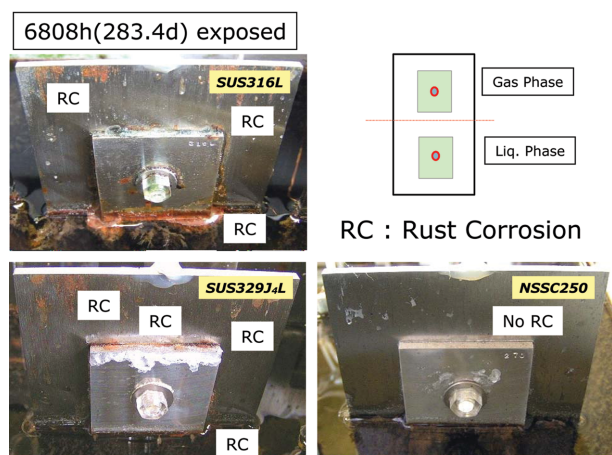


Fig. 21 Conditions of half-exposure test of various stainless steels in natural sea water

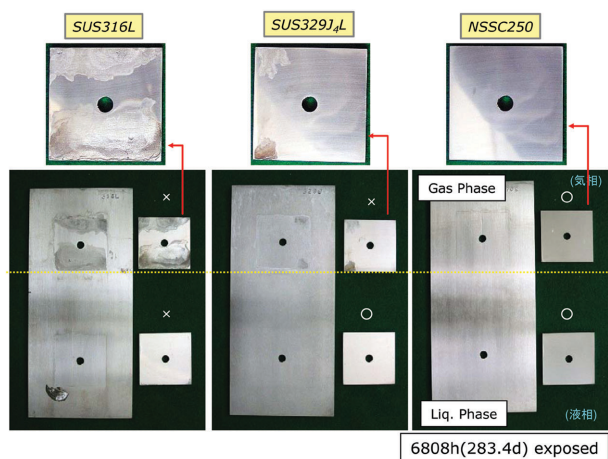


Fig. 22 Corrosion condition of half-exposure test for various stainless steels in natural sea water

strated excellent resistance to crevice corrosion during the period of the present test.

As described above, it was clear from the results of a semi-immersion test in natural seawater that NSSC250 and NSSC270 afforded far superior crevice corrosion resistance to SUS316L and SUS329J₄L.

4. Conclusion

Concerning the crevice corrosion resistance in a seawater-based environment, one of the basic performances of corrosion-resistant stainless steels, we investigated: (1) the natural potential of stainless steel in natural seawater, (2) the corroded crevice repassivation potential associated with the occurrence and growth of crevice corrosion, (3) the time taken before crevice corrosion occurs, and (4) the growth of crevice corrosion, using electrochemical methods in the laboratory, and estimated the service life of various stainless steels subject to crevice corrosion. In addition, we conducted a semi-immersion test of stainless steels in natural seawater. The results we obtained are summarized below.

- 1) The natural potential of stainless steel in river water, lake water and natural seawater is about 440 mV as long as the stainless

steel remains stable in a passive state. This potential corresponds to the natural potential, E_{sp} , that indicates the corrosiveness of the environment (i.e., the environmental force).

- 2) The corroded crevice repassivation potential, $E_{R,CREV}$, that indicates the crevice corrosion resistance of stainless steel is nobler for higher grades of stainless steel (i.e., stainless steels with larger CI values). A comparison between E_{sp} and $E_{R,CREV}$ revealed that in a seawater-based environment, all stainless steels are subject to crevice corrosion eventually (occurrence of crevice corrosion with growth potential).
- 3) The crevice corrosion occurrence time, t_{INC} , for stainless steel was estimated from a current-time curve obtained by the potentiostatic method. The higher the grade (CI value) of stainless steel, the larger the value of t_{INC} becomes. After deliberation on the actual conditions under which stainless steels are used, we concluded that it would be reasonable to set the t_{INC} of SUS304 as 1.0, and indicate the t_{INC} of any other stainless steel in terms of R_{INC} —the value of t_{INC} relative to that of SUS304. According to one report on a stainless steel immersion test in actual seawater, crevice corrosion occurs on SUS304 in about one year. Based on this data, we estimated the crevice corrosion occurrence time (t_{INC}) for various stainless steels in actual seawater from their R_{INC} .
- 4) We studied the growth of crevice corrosion that occurred using the potentiostatic method. The maximum crevice corrosion depth, D_{max} , of stainless steel is proportional to time raised to the second power. Assuming the sheet thickness of a structure as 8 mm, we estimated the time in which the sheet is penetrated by crevice corrosion. The calculated perforation time—the sum of the time at which crevice corrosion begins and the time taken for the crevice corrosion to penetrate the 8-mm-thick sheet—was about 4.67 years for SUS316L, about 484 years for SUS329J₄L, about 1,110 years for NSSC250 and about 3,098 years for NSSC270. Thus, in practical terms, the perforation time for stainless steels of higher grade than SUS316L poses no problem.
- 5) Test pieces having two crevices, one immersed in seawater and one exposed to the air, were subjected to a semi-immersion test for 6,808 hours in a seawater pool into which fresh natural seawater was constantly flowing. With SUS316L and SUS329J₄L, rust or crevice corrosion occurred on at least one of the two crevices. In the case of NSSC250 and NSSC270, by contrast, all the crevices were completely free of rust and damage caused by crevice corrosion during the period of the present test.

References

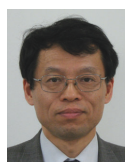
- 1) ASTM Standards, G78-83. ASTM, Philadelphia, 1983
- 2) Kain, R.M.: Corrosion. 40, 313 (1984)
- 3) Kain, R.M., Lee, T.S., Oldfield, J.W.: Corrosion/85. NACE, Boston, Paper No.60, 1985
- 4) Streicher, Michael A.: Materials Performance. 22, 37 (1983)
- 5) ASTM Standards, G48-79. ASTM, Philadelphia, 1979
- 6) Kain, R.M.: Corrosion/79. NACE, Atlanta, Paper No.230, 1979
- 7) Japanese Standards Association: Method of Determining the Repassivation Potential for Crevice Corrosion of Stainless Steels. JIS G 592:2002, 2002
- 8) Tsujikawa, S., Hisamatsu, K.: Boushoku-Gijutsu (Presently Zairyo-to-Kankyo). 29, 37 (1980)
- 9) Akashi, M., Tsujikawa, S.: Zairyo-to-Kankyo. 45, 106 (1996)
- 10) JSCE: Zairyo Kankyo-Gaku Nyuumon. Maruzen, 1993, p.31
- 11) Shinohara, T., Tsujikawa, S., Mashiko, N.: Boushoku-Gijutsu (Presently Zairyo-to-Kankyo). 39, 238 (1990)
- 12) Shinohara, T., Fukaya, Y.: Proc. 52nd Jpn. Conf. Materials and Environments. JSCE, 2005, p.399

NIPPON STEEL TECHNICAL REPORT No. 99 SEPTEMBER 2010

- 13) Fukaya, Y., Shinohara, T.: Proc. 52nd Jpn. Conf. Materials and Environments. JSCE, 2005, p.403
14) Tomari, H.: Proc. 62nd Symposium. JSCE, 1985, p.40
15) Public Works Research Institute Data No.3686: Guidelines on Prevention of Corrosion of River/Dam Facilities (Draft). Stainless Steel Materials Volume. 2000
16) Suutala, N., Kurkela, M.: Stainless Steels '84. NACE, 1984, p.240
17) Ito, K., Matsuhashi, R., Kihira, H.: Proc. 125th Symposium. JSCE, 2000, p.5
18) Ogawa, H., Ito I., Nakada, M., Hosoi, Y., Okada, H.: Tetsu-to-Hagané. 23, 605 (1977)



Ryo MATSUHASHI
Senior Researcher, D.Eng., Steel Products Research
Lab. - I, Steel Research Laboratories,
Nippon Steel Corporation
20-1, Shintomi, Futtsu, Chiba



Shinji TSUGE
Chief Researcher,
Steelmaking, Plate, Bar & Wire Rod Research & Development Div., Research & Development Center,
Nippon Steel & Sumikin Stainless Steel Corporation



Yutaka TADOKORO
Senior Researcher,
Steelmaking, Plate, Bar & Wire Rod Research & Development Div., Research & Development Center,
Nippon Steel & Sumikin Stainless Steel Corporation



Tooru SUZUKI
Senior Manager, Technical Div.,
Nippon Steel & Sumikin Stainless Steel Corporation